Eur. Phys. J. A **25**, s01, 263–266 (2005)
DOI: 10.1140/epjad/i2005-06-138-5

EPJ A direct
electronic only

Reactions induced beyond the dripline at low energy by secondary beams

W. Mittig[1,a], C.E. Demonchy[1,5], H. Wang[1,b], P. Roussel-Chomaz[1], B. Jurado[1,c], M. Gelin[1], H. Savajols[1], A. Fomichev[2], A. Rodin[2], A. Gillibert[3], A. Obertelli[3], M.D. Cortina-Gil[4], M. Caamaño[4], M. Chartier[5], and R. Wolski[6,d]

[1] GANIL (DSM/CEA, IN2P3/CNRS), BP 5027, 14076 Caen Cedex 5, France
[2] FLNR, JINR, P.O. Box 79, 101 000 Dubna, Moscow region, Russia
[3] CEA/DSM/DAPNIA/SPhN, Saclay, 91191 Gif-sur-Yvette Cedex, France
[4] University of Santiago de Compostela, E-15706 Santiago de Compostela, Spain
[5] University of Liverpool, Department of Physics, Oliver Lodge Laboratory, Liverpool L69 7ZE, UK
[6] Institute of Nuclear Physics PAN, Radzikowskiego 152, PL-31-342, Cracow, Poland

Received: 15 January 2005 /
Published online: 12 July 2005 –

Abstract. Reactions induced on protons at low incident energy (3.5 MeV/n) were measured with a ^{8}He beam accelerated by Spiral at Ganil. The particles were detected in the active target Maya, filled with C_4H_{10} gas. The beam was stopped in the detector, so energies from incident beam energy down to detector threshold were covered. Proton elastic scattering, one neutron pick-up (p, d) and (p, t) reactions were observed. In the (p, d) reaction very high cross-sections of the order of 1barn were observed, that could be reproduced using a direct reaction formalism. This is the first time that this strong increase of transfer reaction cross-sections at very low energy predicted for loosely bound systems was observed. Spectroscopic factors are in agreement with a simple shell model configuration. No evidence for a low lying excited state in ^{7}He was found.

PACS. 24.50.+g Direct reactions – 29.40.-n Radiation detectors

1 Introduction

Since 1989 low energy reaccelerated secondary beams are available at LLN, and in more recent years at Ganil-Spiral, ORNL, Triumf-Isac and Rex-Isolde with energies typically in the 0.1–10 MeV/n domain. These energies are ideally suited for the study of resonant reactions, among them those of astrophysical interest, and direct transfer or pick-up reactions. Elastic and inelastic scattering are other reactions of interest at this energy, especially near or below the Coulomb barrier. In most of these studies the interaction with simple target nuclei, such as protons, deuterons, ^{3}He and ^{4}He is preferred in order to obtain quantitative results. A recent review on this subject can be found in ref. [1]. A detector, in which the detector gas is the target, this is, an active target, has in principle a 4π solid angle of detection, and a big effective target thickness without loss of resolution, and is thus ideally suited for the study of reactions induced by reaccelerated secondary beams from Spiral at Ganil in the energy domain of 2–25 MeV/n. The detector developped, called Maya, used isobutane C_4H_{10} as gas in the first experiments, and other gases such as D_2. The multiplexed electronics of more than 1000 channels allows the reconstruction of the events occurring between the incoming particle and the detector gas atoms in 3D. Here we will present mainly reactions induced by ^{8}He on protons at 2–3.5 MeV/n. The design of the detector is shown, and some first results are discussed.

2 The Maya detector

Active targets, such as bubble chambers were developped since a long time in high energy physics. In the domain of secondary beams, the archetype is the detector IKAR [2]. A discussion of the use of this detector for elastic scattering at GSI energies can be found in ref. [3]. The use of IKAR was limited to H_2 at a pressure of 10 atm. Another example can be found in ref. [4], where a flash ADC readout of wedge signals was used. For the domain of low energies, and for the use of various gases, we developped a new detector called Maya [5,6] that we will describe here. The detector is shown schematically in fig. 1.

[a] Conference presenter; e-mail: mittig@ganil.fr
[b] *Present address*: IMP Lanzhou, PRC.
[c] *Present address*: CENBG Bordeaux, France.
[d] Partially supported by the IN2P3-Poland cooperation agreement 02-106.

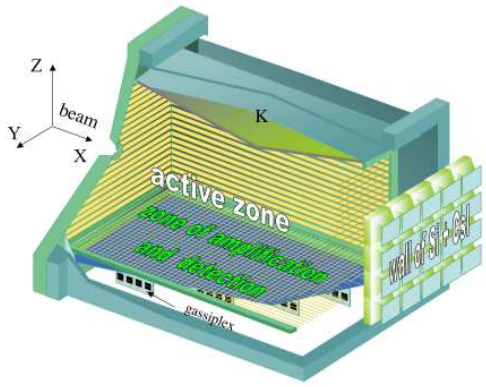

Fig. 1. The scheme of the detector Maya. The secondary beam is incident from the left, the electrons produced by ionising reaction products in the detector gas drift down, and induce a signal after amplification in the honeycomb like anode pattern. These signals are read out by Gassiplex electronics below this anode.

For a two body reaction, scattered and recoiling particles are in a plane. The electrons from the ionisation of the gas by the particles are drifting down in the electric field to the amplifying wires. The wires are parallel to the beam. Therefore their diameter can be different in the region of the beam, to adjust for different ionisation densities of beam and recoil particles. In an experiment with ^{8}He, we obtained a gain of 1/10 in this central region by the use of 20 μm instead of 10 μm amplifying wires. The spacing of the wires should be quite small, in principle less than the drift straggling of the electrons in order to avoid digitalisation. We used a distance of 3 mm. The wires corresponding to a line of pads are connected to the same preamplifier. The angle of the reaction plane can be determined by the drift time to the wires. The amplified signal is induced in the pads below. The distance between the wires and the pads determines the width of the induction pattern. A distance of 10 mm was chosen in order to have the best position resolution that is obtained when the signal of the two nearby lateral pads have about half the amplitudes of a central pad. A hexagonal structure was chosen for these strips, in order to have best conditions for the reconstruction of the trajectory, independant of the direction. This results in a honeycomb structure. A matrix of 35 by 34 pads, this is 1190 pads, constitutes this anode. The pads are arranged in rows below the wires, in order to have a precise time relation between the wire signal and the pad signal. The pads are connected to Gassiplex. The Gassiplex chip is a 16 analogical multiplexed channel ASIC developed at CERN. The multiplexed readout limits the number of connections from the detector to the outside. The Gassiplex are mounted on the back of the anode. The Gassiplex need a track and hold signal, provided by the wire signal, treated by classical electronics. The detector can be characterized as a CPC: Charge Projection Chamber in analogy with time projection chambers TPC.

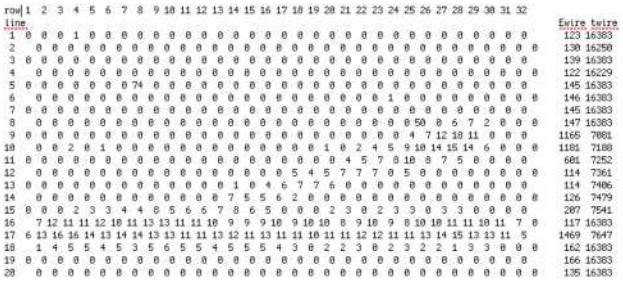

Fig. 2. Typical event matrix as read out for the Maya detector. The calibrated amplitude (in channels/10) from the Gassiplex matrix is printed out for the 32 rows, and the first 20 lines. The beam particle is coming from the left, identified as ^{23}F, and makes a (d, ^{3}He) reaction after about one third of the length of the detector. The signal amplitudes in the wire lines and the respective times are printed out on the right.

A typical event read-out matrix is shown in fig. 2. It was observed with a cocktail beam around ^{26}F at about 30 MeV/nucleon. In this case the detector was filled with pure D_2 to observe the (d, ^{3}He) reaction. The last column gives the drift times from TDC's, and as can be seen, the ^{3}He particle is going down, the drift times at the end of the trace being smaller than at the beginning. The number 16383 means that the corresponding TDC had not fired. The determination of the trajectories in 3 dimensions from readout matrices as shown in fig. 2 needed a quite important development of software [6].

As pointed out above, inverse kinematics generate recoil particles in a large energy domain. High energy light particles such as protons cannot be stopped in a reasonable gas volume. For escaping particles, we added a Si-CsI wall of $20 \times 25\,\mathrm{cm}^2$, covering about 45 degrees around the beam for events in the middle of the detector. The detectors have an area of $5 \times 5\,\mathrm{cm}^2$. The thickness of the Si detectors is 500 μ and 1 cm for the CsI. For particles stopping in the gas, identification is obtained by the total charge-range correlation. For events stopping in the Si, the energy loss in the gas is used for dE-E identification. For elastic scattering a matrix for the correlation of the range of the heavy reaction partner and the energy in one of the Si-detectors is shown in fig. 3. From the width of this correlation and the distance between the two kinematic lines we obtain an excitation energy resolution of 160 keV(FWHM). Note that in the case of a standard thick target, only the projection on the Si-energy axis would be available, and thus would correspond to a complete loss of the information on excitation energy.

3 Results for the ^{8}He(p, d)^{7}He reaction

We present mainly results from an experiment run in july 2004 with a beam energy of 3.5 MeV/n and the detector filled with 0.5 atm of isobutane. With this gas density and this energy, the beam was stopped in the detector, and thus the energy domain covered is between the incident energy and zero energy. First results are given below, and we will show some results of the ^{8}He(p, d) reaction.

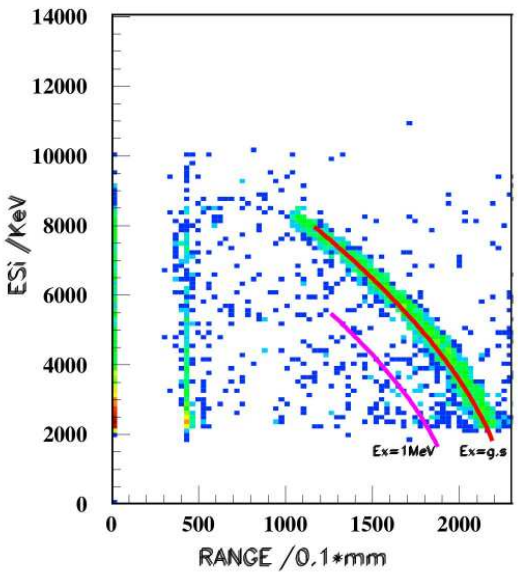

Fig. 3. Scatter plot for particles leaving the gas volume, conditioned by the identification of protons, of the energy deposited in one of the Si-detectors, as a function of the range of the heavy reaction partner measured inside the gas. The two lines represent kinematical calculations for elastic scattering of ^{8}He on protons, and a (hypothetical) excited state at 1 MeV above the ground state.

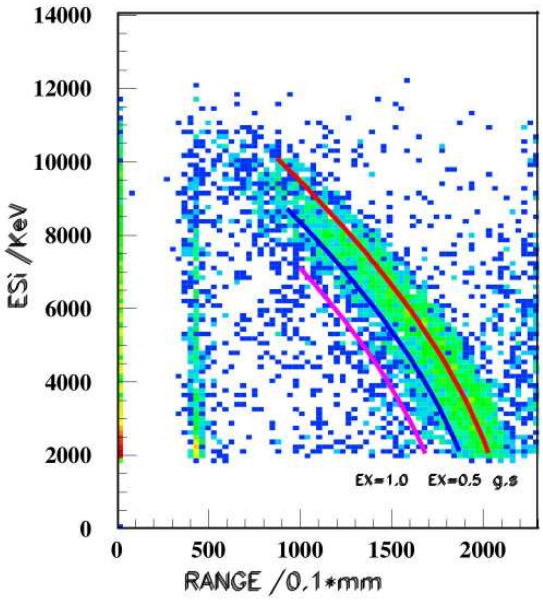

Fig. 4. Scatter plot for particles leaving the gas volume, conditioned by the identification of deuterons, of the energy deposited in one of the Si-detectors, as a function of the range of the heavy reaction partner measured inside the gas. The three lines represent kinematical calculations for the (p, d) leading to the unbound groundstate of ^{7}He and to excited states at 0.5 and 1 MeV above the ground state. As can be seen by comparison with fig. 3, the width of the distribution is essentially due to the finite width of the states in ^{7}He.

3.1 Analysis of the energy spectrum of the ^{8}He(p, d)^{7}He reaction

The ground state of ^{7}He is known [7] to be unbound by 440 keV, with a width of 150 keV. Thus ^{7}He disintegrates in ^{6}He plus neutron, and the remaining ^{6}He has a variable kinetic energy due to recoil. The broadening of the resolution function as compared to the elastic scattering (see fig. 3), and as observed for the ^{8}He(p, t)^{6}He$_{gs}$ (not shown), is evident in fig. 4. This broadening is due to the intrinsic width of the unbound states in ^{7}He. In a fragmentation reaction at GSI [8], evidence for a state at (0.6±0.1) MeV above ground state was found with a width of (0.75 ± 0.08) MeV. Such a state would be of great interest, since it could be the $p^{-}_{1/2}$ spin-orbit partner of the $p^{-}_{3/2}$ ground state, and would indicate a strong quenching of the spin-orbit strength far from stability.

In ref. [9] an excited state at 2.9 ± 0.3 MeV (Γ = 2.2 ± 0.3 MeV) was observed. In heavy ion transfer reactions [10], only the ground state of ^{7}He was observed. In a more recent experiment [11], in the ^{9}Be(^{15}N, ^{17}F)^{7}He reaction excited states were observed at 2.95 ± 0.1 MeV (Γ = 1.9 ± 0.3 MeV), in very good agreement with ref. [9], and (5.8 ± 0.3) MeV (Γ = 4 ± 1 MeV). Very recently [12], the authors concluded that this low lying state does not exist in an experiment on the isobaric analogue state of ^{7}He. In an analysis using the recoil corrected continuum shell model [13], it was argued that at the experimental angle of 180 degrees of ref. [12] the effect of such a resonance would be very small. Theoretical models, such as nocore SM, QMC, resonating group model, or shell model with different configuration spaces predict a $p_{1/2^-}$ state at typically 2–4 MeV above ground state.

The extraction of information on excited states in ^{7}He from experimental spectra is complicated by the fact that the widths are large, and the width and the population cross-section are strongly energy dependent. We treated the energy dependance of the decay width in two ways with very similar results. One was the energy dependance as cited in ref. [11], the other was the calculation of single particle resonance width by the code Fresco [14]. The result can be described to a good approximation by the simple formula $\Gamma(E) = \Gamma_r * E/E_r$. In fig. 5 this relation was used. The population cross-section was calculated as a function of excitation energy using the code Fresco. We included in the fit the following resonances: $E_r = 0.44$ MeV with $\Gamma_r = 0.15$, $E_r = 1.00$ MeV with $\Gamma_r = 0.75$ MeV, and $E_r = 3.3$ MeV with $\Gamma_r = 2.0$. The energy of the center of the last resonance is below threshold for the present experiment, however the tail extends to low excitation energies. The energy spectrum, as projected from fig. 4 on the Si-energy axis, was simulated in a Monte-Carlo method. The experimental energy resolution being much better than the observed structure, it was not necessary to take it into account in the simulation. The individual contributions for these 3 resonances are shown, with arbitrary normalization, in fig. 5. The final fit is shown as solid line. In this fit the contribution relative to the ground

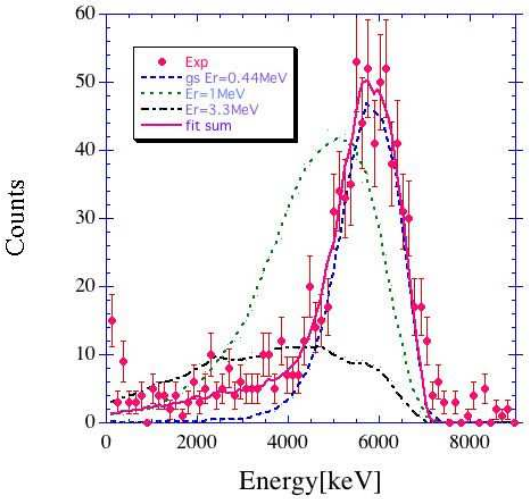

Fig. 5. Projected energy spectrum for the (p, d) reaction. The experimental count rate/energybite are compared to a Monte-Carlo simulation of this spectrum, including the effect of the energy dependant decay width, recoil broadening, energy dependance of the population cross-section. The individual contribution, with arbitrary normalisations, are shown for the ground state, a hypothetical state at 1 MeV separation energy, and a state at 3.3 MeV separation energy. The fitted sum of these contributions is shown, too. For details see text.

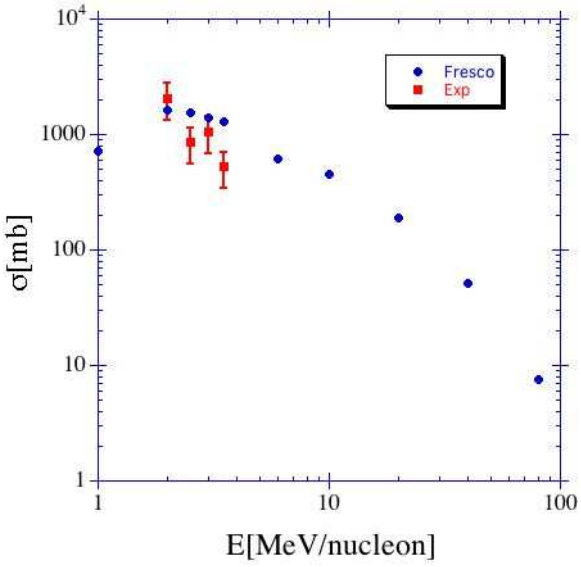

Fig. 6. Angle integrated cross-section for the $^{8}\mathrm{He}(\mathrm{p},\mathrm{d})^{7}\mathrm{He}_{gs}$ reaction. The theory is given for $C^2S = 4$.

state for the state at $E_r = 1\,\mathrm{MeV}$ was (-0.015 ± 0.082). This means no contribution of such a state is seen, and the upper limit is far below the 30% contribution of ref. [8].

3.2 Reaction cross-sections of the $^{8}\mathrm{He}(\mathrm{p},\mathrm{d})^{7}\mathrm{He}_{gs}$ reaction

The angular distributions were obtained for maximum energy down to about 2 MeV/n. They were analysed using the code Fresco, with an optical potential taken from CH89 [15]. Experimental uncertainties of the absolute cross-section are of the order of 30% due to efficiency of the reconstruction algorithm. The optical model introduces another uncertainty in the evaluation of this reaction. Nonetheless, the angular distributions agree well, and a spectroscopic factor $C^2S = 3 \pm 1$ is obtained in the analysis. This is close to a simple shell model estimation where one expects $C^2S = 4$ for 4 nucleons in the $p_{3/2}$ shell. A similar result was obtained at much higher energy [9].

Large transfer reaction cross-sections have been predicted at low energy for loosely bound systems [16]. This results from the very low Fermi momentum of the loosely bound last nucleons in these systems, which implies highest overlap at very low velocity. To our knowledge this effect has not yet been observed. In fig. 6 the angle integrated cross-section as a function of energy is shown. The experimental data were integrated using the Fresco angular distributions renormalized on the experimental data. As can be seen, the cross-section is very high, reaching 1barn in the energy domain of the present experiment. The good agreement between the theory and experiment shows that even at this low energy the direct reaction mechanism may account for the observed cross-sections.

The results shown here, and results on elastic scattering and the (p, t) reaction that were observed simultaneously and which will be discussed elsewhere, illustrate the interest of secondary beams at low energy. An active target as the MAYA detector presented is a powerful tool in this domain.

References

1. P. Roussel Chomaz *et al.*, Nucl. Phys. A **693**, 495 (2001).
2. A.A. Vorobyov *et al.*, Nucl. Instrum. Methods **119**, 509 (1974); Nucl. Instrum. Methods A **270**, 419 (1988).
3. P. Egelhof, *Proceedings of the International Workshop on Physics with Unstable Nuclear Beams, Serra Negra, Sao Paulo Brazil*, edited by C.A. Bertulani *et al.* (World Scientific, 1997) p. 222.
4. Y. Mizoi *et al.*, Nucl. Instrum. Methods A **431**, 112 (1999); Phys. Rev. C **62**, 065801 (2000).
5. P. Gangnant *et al.*, report Ganil 27.2002.
6. C.E. Demonchy, thesis T 03 06, December 2003, University of Caen, France.
7. D.R. Tilley *et al.*, TUNL Manuscript, *Energy levels of light nuclei A = 7, and Energy levels of light nuclei A = 9.*
8. M. Meister *et al.*, Phys. Rev. Lett. **88**, 102501 (2002).
9. A.A. Korsheninnikov *et al.*, Phys. Rev. Lett. **82**, 3581 (1999).
10. W. von Oertzen *et al.*, Nucl. Phys. A **588c**, 129 (1995).
11. H.G. Bohlen *et al.*, Phys. Rev. C **64**, 024312 (2001).
12. G.V. Rogachev *et al.*, Phys. Rev. Lett. **92**, 232502 (2004).
13. D. Halderson, Phys. Rev. C **70**, 041603R (2004).
14. I.J. Thompson, Comput. Phys. Rep. **7**, 167 (1988).
15. R.L. Varner *et al.*, Phys. Rep. **201**, 57 (1991).
16. H. Lenske, G. Schrieder, Eur. Phys. J. A **2**, 41 (1997).